

Journal of Optoelectronical Nanostructures



Autumn 2025 / Vol. 10, No. 3: 88-101

Calculation of the energy eigenvalue and linear refractive index changes and intersubband optical absorption coefficients in a Confineme quantum dot with a potential

Mohsen Bagheri, Heydar Izadneshan*,1, Ghahraman Solookinejad1

¹ Department of Physics, Marvdasht Branch, Islamic Azad University, Marvdasht, Iran

Received: 2025.03.02 Revised: 2025.10.16 Accepted: 2025.10.18 Published: 2025.11.30

Use your device to scan and read the article online.



Keywords:Quantum dot energy eigenvalue, Nonlinear and linear

optical properties

Abstract

In this study, a comprehensive analysis of the electronic energy spectrum and refractive index variations in semiconductor quantum dots is presented. Using the matrix formalism, the relationship between the linear refractive index and carrier concentration is systematically derived. calculations carried Numerical are GaAs/Al_xGa_{1-x}As quantum dot heterostructure to explore how optical excitation intensity, dot size, and alloy composition influence the energy levels and optical response. The results demonstrate that these parameters significantly modify both the electronic structure and optical coefficients, including the linear, nonlinear, and third-order absorption behaviors. These coefficients are further examined as functions of photon energy and incident optical field intensity, exhibiting characteristics similar to those observed in quantum wells. Notably, the enhanced absorption within the visible and infrared regions highlights the strong potential of such quantum dots for advanced optoelectronic devices, particularly high-efficiency photodetectors, lasers, and solar energy conversion systems.

Citation: Mohsen Bagheri, Heydar Izadneshan, Ghahraman Solookinejad, Calculation of the energy eigenvalue and linear refractive index changes and intersubband optical absorption coefficients in a Confineme quantum dot with a potential. **Journal of Optoelectronical Nanostructures.** 2025; 10 (3): 88-101.

*Corresponding author: Heydar Izadneshan

Address: Department of Physics, Marvdasht Branch, Islamic Azad University, Marvdasht, Iran

Email: izadneshan@miau.ac.ir

DOI: https://doi.org/10.71577/jopn.2025.1200949

1. Introduction

Over the past few decades, quantum dot (QD) nanostructures have been extensively studied due to their unique physical properties and wide potential in emerging technologies. These systems have drawn remarkable attention in both fundamental physics and chemistry, particularly for their applicability in optoelectronic devices [1]. Examples of such applications include semiconductor lasers [2], single-electron transistors [2], quantum information processing [4, 5], optical data storage [6], mobile communication technologies [7], and infrared detection systems [8]. The pioneering concepts of quantum wires and quantum dots were first introduced by Esaki and Tsu in the 1970s [9]. In specific configurations, ODs are able to emit radiation in the terahertz frequency regime [25], which is highly attractive for imaging, aerospace, defense, and medical applications [26]. Among the broad range of semiconductor technologies, solar cells represent one of the most impactful innovations, being widely adopted for large-scale power generation [28, 29]. With the progress of modern materials science, it has become feasible to fabricate low-dimensional systems capable of confining carriers in one, two, or all three spatial directions. This has stimulated growing interest in investigating optical transitions between subbands in quantum-confined semiconductors. Owing to their large dipole matrix elements and resonance conditions, both linear and nonlinear optical processes have been extensively addressed in such systems [10–13]. For instance, Kan et al. [19] presented theoretical studies on how absorption and refractive index vary with inter-subband transitions in single and multiple quantum wells. Likewise, Chuang and collaborators [21] examined the influence of external electric fields on optical absorption and refractive index behavior in heterostructures with parabolic confinement. In the present study, we provide an analytical framework to calculate the energy eigenvalues of quantum dots and investigate the effect of structural parameters, such as size and alloy composition, on inter-subband refractive index changes. For this purpose, a finite-potential quantum dot model is employed.

Comsol applications are basically a complete simulation suite that can be used in a simulation environment, for Graphics of differential equations using the finite element method (Finite Element Method); FEM to solve. The fields of use of this simulator are very wide. Problems of physics, optics, electrochemistry, heat and fluids, Plasma, radio waves, acoustics, and various types of issues that exist in three-dimensional or less-dimensional space. They can be defined and simulated in these applications. The implementation of the software is such that this software uses the FEM method to solve basic electrostatic and magnetic equations, with boundary conditions and space that you will determine according

to your problem. In this way, space 3D is divided into a large number of meshes, and each mesh is considered as a partial element.

Then the desired equations are generalized to these components, and thus variables such as flood potential, field Electric, electric displacement, etc. will be calculated in the whole space [25].

COMSOL is an advanced multiphysics simulation platform that offers a comprehensive environment for modeling and solving differential equations through the Finite Element Method (FEM). It supports a wide range of applications, enabling the simulation of complex phenomena in fields such as physics, optics, electrochemistry, heat transfer, fluid dynamics, plasma physics, radio frequency analysis, acoustics, and more. These simulations can be carried out in one, two, or three-dimensional geometries [25]. In this study, COMSOL is employed to analytically determine the energy eigenvalues of quantum dots. The simulation explores how variations in structural parameters—such as the dot size and material composition ratio—affect changes in the inter-subband optical refractive index of the quantum dot. For this purpose, a quantum dot with finite potential confinement is modeled. The geometric structure of the quantum dot used in the simulation is illustrated below.

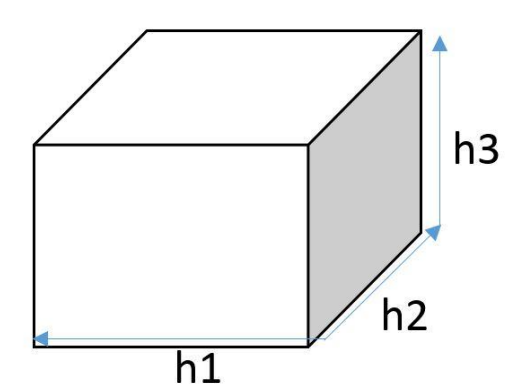


Fig.1. Geometry structure of quantum dot (h_1, h_2, h_3)

2. MATH

In the first step, we simulate the quantum dot with the help of Comsol applications, and then we get the specific values of energy and specific values of functions. In the second step, we change the size of the quantum dot and obtain the specific energy values and specific functions for its different sizes. In the third step, with the help of the data obtained from the Comsol applications, we obtain the absorption coefficient and the linear and non-linear refractive index for the quantum dot and examine their figure. At the end, we calculate the absorption coefficient and the total refractive index for the quantum dot and examine its figure.

2.1 EQUATIONS

The electron Hamiltonian for the quantum dot system is given by:

$$H = -\frac{\hbar^2}{2m^*} \nabla^2 + V(r) \tag{1}$$

Where m^* is the effective mass and V(r) the confining potential:

$$V(r) = \begin{cases} 0 & input \\ V_0 & output \end{cases}$$
 (2)

In Equation (2), V_0 represents the potential barrier between GaAs and $Al_xGa_{1-x}As$, which is expressed in terms of the band-gap discontinuity DE_G . It is assumed that the barrier height is o. 60% of the total band-gap difference between the two materials. For the $GaAs/Al_xGa_{1-x}As$ heterostructure, the band-gap discontinuity is given by the relation $DE_G = 1.04x + 0.47x^2$ (eV), where X denotes the aluminum concentration. The ground state wave function of the quantum dot is modeled accordingly, and the associated special functions have been computed using numerical methods.

2.2 OPTICAL PROPERTIES

The ground state wave function in a quantum dot takes the form:

$$\psi(x, y, z) = N \varphi_1(x)\varphi_1(y)\varphi_1(z) \tag{3}$$

By solving the Schrödinger equation for the given quantum dot system, the wave functions are expressed in terms of Bessel functions. Similar forms are utilized for $j_1(y)$ and $j_1(z)$. In this study, optical transitions between two subbands within the conduction band are examined. Specifically, we evaluate the linear and nonlinear absorption coefficients, as well as changes in the refractive index,

arising from an optical transition between the ground state $n_x = n_y = n_z = 1$ and an excited state $n_x = 2$, $n_y = n_z = 1$. The wave functions corresponding to this excited state are also determined. To compute variations in the refractive index and absorption coefficients resulting from this inter-subband transition, we apply the compact-density formalism. The quantum dot structure is subjected to an external electromagnetic field, which induces the optical transitions under investigation as [17]:

$$E(t) = E_0 \cos(\omega t) = \tilde{E} e^{i\omega t} + \tilde{E} e^{-i\omega t}$$
(4)

The analytical forms of the linear $\chi^{(1)}$ and $\chi^{(3)}$ susceptibilities are obtained as follows. First, for the linear term,[17]

$$\varepsilon_0 \chi^{(1)}(\omega) = \frac{\sigma_V |M_{21}|^2}{E_{21} - \hbar \omega - i\hbar \Gamma_{12}}$$
 (5)

$$\varepsilon_{0}\chi^{(3)}(\omega) = -\frac{\sigma_{V} |M_{21}|^{2}|E|^{2}}{(E_{21} - \hbar\omega - i\hbar\Gamma_{12})} \times \frac{4|M_{21}|^{2}}{(E_{21} - \hbar\omega)^{2} - (i\hbar\Gamma_{12})^{2}} - \frac{(M_{22} - M_{11})^{2}}{(E_{21} - i\hbar\Gamma_{12})(E_{21} - \hbar\omega - i\hbar\Gamma_{12})}$$
(6)

The susceptibility w (o) is related to the change in the refractive index as follows [23]:

$$\frac{\Delta n(\omega)}{n_r} = Re \frac{\chi(\omega)}{2n_r^2} \tag{7}$$

Where n_r is the refractive index. By using Eqs. (14–15), the linear and third-order nonlinear refractive index changes are obtained by:

$$\frac{\Delta n^{1}(\omega)}{n_{r}} = \frac{1}{2n_{r}^{2}\varepsilon_{0}} \sigma_{V} |M_{21}|^{2} \frac{E_{21} - \hbar\omega}{(E_{21} - \hbar\omega)^{2} - (i\hbar\Gamma_{12})^{2}}$$
(8)

And

$$\frac{\Delta n^3(\omega)}{n_r} = -\frac{1}{4n_r^3 \varepsilon_0} \frac{\sigma_V I}{[(E_{21} - \hbar \omega)^2 - (i\hbar \Gamma_{12})^2]^2} \times [4((E_{21} - \hbar \omega)|M_{21}|^2)]$$

$$-\frac{(M_{22}-M_{11})^2}{(E_{21})^2-(i\hbar\Gamma_{12})^2}\{(E_{21}-\hbar\omega)\times[(E_{21}\times(E_{21}-(\hbar\Gamma_{12})^2(2E_{21}-\hbar\omega))\}\ (9)$$

Where σ_V is the carrier density in this system, m is the permeability of the system, $E_{ij} = E_i - E_j$ is the energy interval of two different electronic states, M_{ij} is the matrix elements, which is defined by $M_{ij} = |\langle \varphi_i | qz | \varphi_j \rangle|$ [17].

The subsequent section presents graphical representations of the computed energy levels, reflection coefficients, and both linear and nonlinear changes in the refractive index. The energy states of the quantum dot have been determined through numerical simulation methods using specialized software tools. The focus of the analysis is a GaAs/Al_{1-x}Ga_xAs semiconductor quantum dot system, modeled with a finite confinement potential of V_0 =0.6 eV, and we used $\sigma_V = 3 \times$ $10^{16} cm^2$, $n_r = 3.2$, $T_{12} = 0.2$, $T_{12} = \frac{1}{T_{12}}$. This study examines how both linear and nonlinear refractive index coefficients respond to changes in structural and optical parameters. In our simulations, it is assumed that the static dielectric constant $\varepsilon = 13.18$) remains uniform across both GaAs and Al_xGa_{1-x}As materials. However, the effective mass of the charge carriers is considered different: $m_1 = 0.067m_0$ is assigned to the GaAs region (quantum dot), and $m_2 = (0.067 + 0.083 \text{x}) m_0$ to the surrounding barrier material (Al_xGa_{1-x}As). The aluminum composition used in the calculations is x = 0.30, and the quantum dot is subjected to a specific incident optical intensity to evaluate its optical response.

3. GUIDELINES FOR GRAPHICS PREPARATION AND SUBMISSION

The following are graphics related to the quantum dots under consideration. Graph 2: In Figure 2, quantum dot energy for 6 different sizes, h_1 =10nm, h_2 =20nm, h_3 =variable, is plotted in a diagram as follows. As can be seen from the graph, the quantum dot decreases with increasing magnitude.

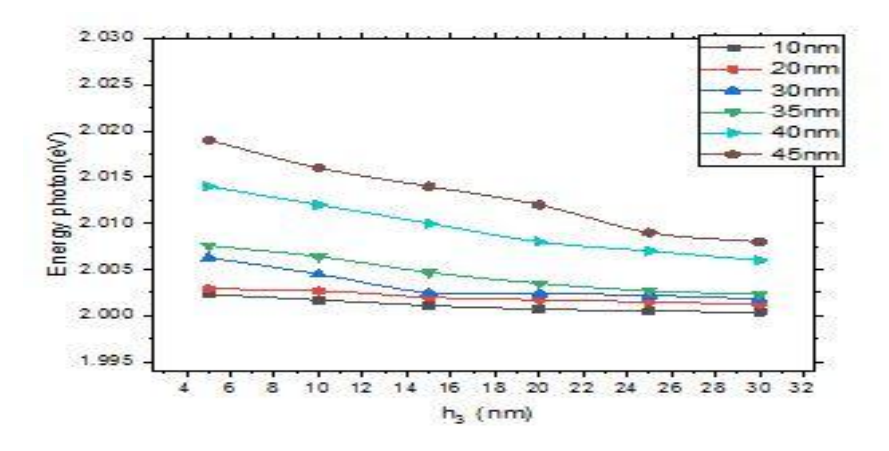


Fig.2. Special diagram of energy values according to size for different sizes h3 (along the z axis)

Graph 3:

In Fig. 3, the linear refractive index changes are plotted as a function of the photon energy for different sizes h3 (along the z axis), as shown below. Therefore, the refractive index change will be reduced. Thus, the calculation of the refraction index change using only the linear w(1) term may not be correct for systems operating, especially with a high optical intensity, because of the strong dependence of w(3) on the incident optical intensity.

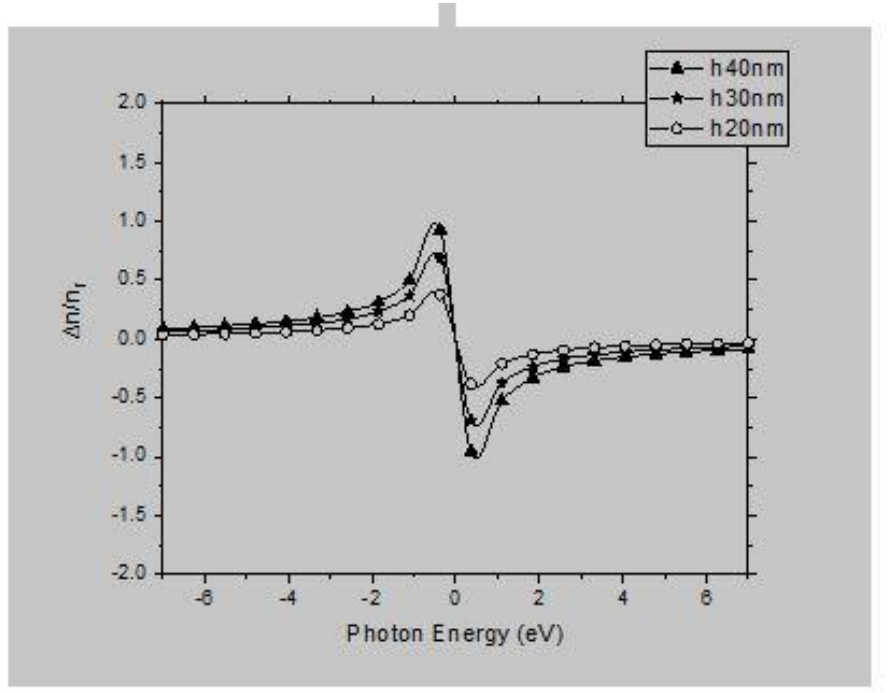


Fig. 3. The variation of the linear index change with the photon energy values for different sizes h3 (along the Z axis)

Graph 4:

In Fig.4, the nonlinear refractive index as a function of photon energy for different sizes h3 (along the z axis) is as follows. As can be seen, with the increase in the size of the quantum dot, the energy decreases and the refractive index increases.

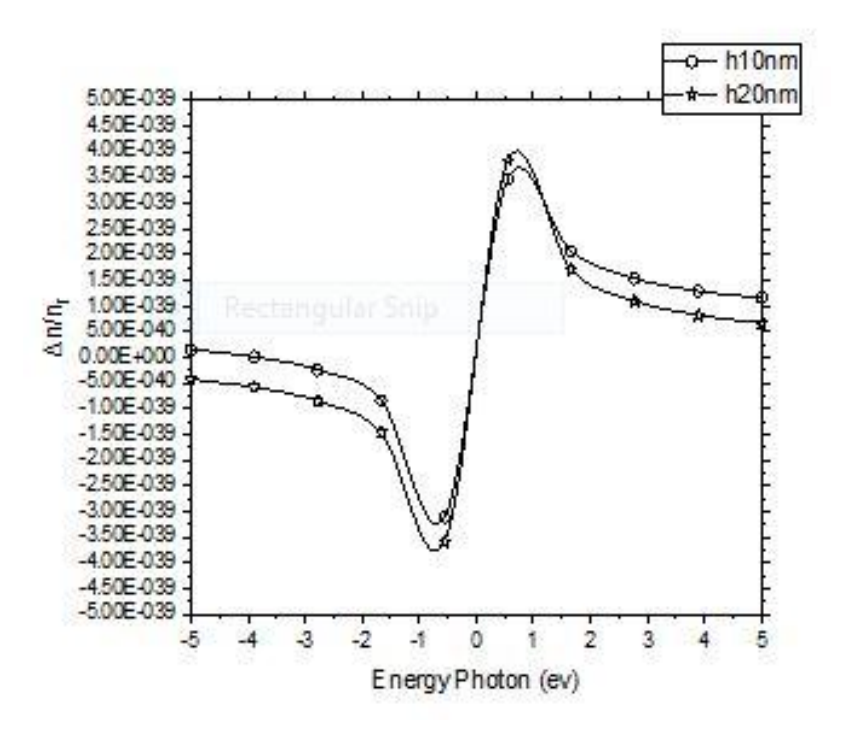


Fig. 4. The variation of the nonlinear refractive index change with the photon energy values, different sizes h3 (along the Z axis)

Graph 5:

In Figure 5, the linear and non-linear refractive index, as well as the total refractive index in terms of photon energy for different sizes h3 (along the z axis), are shown below. We know that the total refractive index is the sum of the linear and non-linear refractive indices. As can be seen, with the increase in the size of the quantum dot, the energy decreases and the refractive index increases.

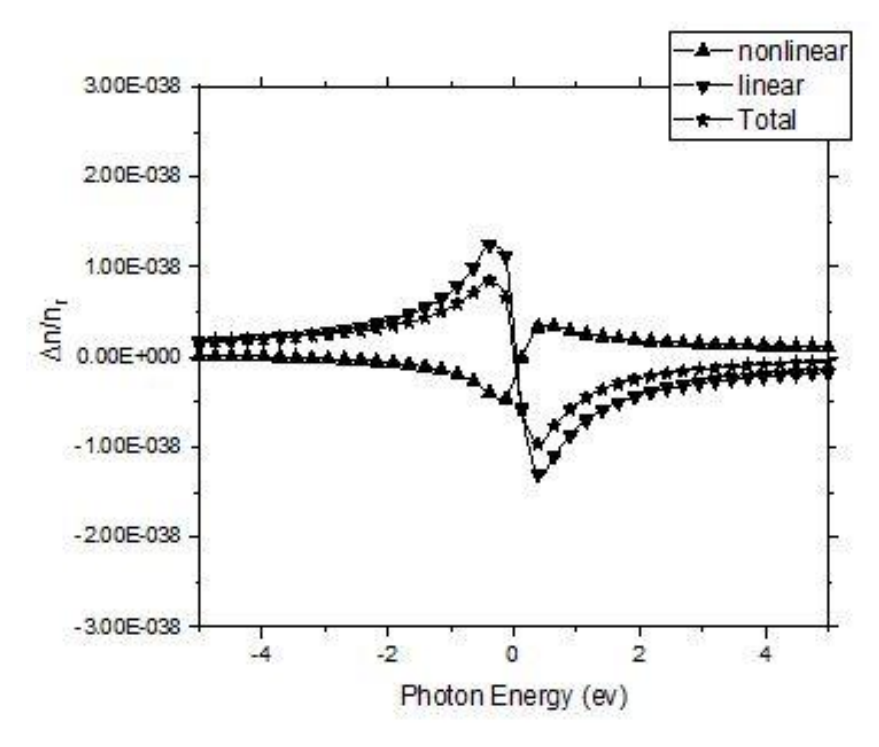


Fig. 5. The variation of the linear, third linear, and total refractive index change with the photon energy values for different sizes h3 (along the Z axis)

Graph 6:

In Figure 6, the graph of the nonlinear absorption coefficient in terms of photon energy for different sizes h3 (along the z axis) is shown below. As can be seen, with the increase in the size of the quantum dot, the energy decreases, and the absorption coefficient decreases.

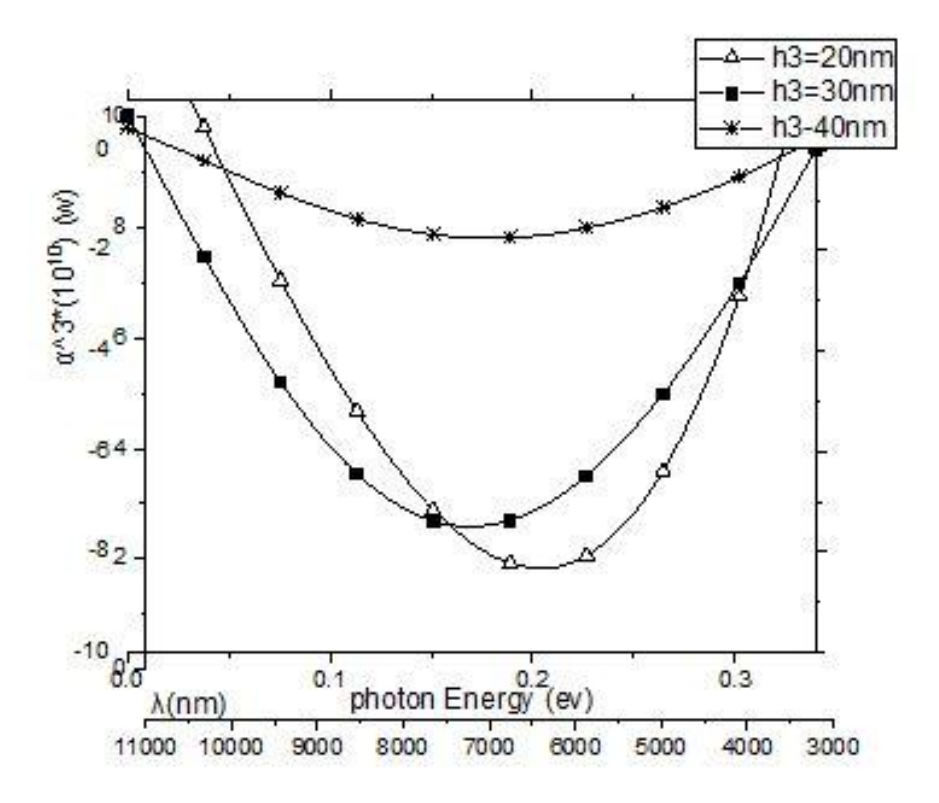


Fig. 6. The variation of the nonlinear absorption coefficients with the photon energy values for different sizes h3 (along the Z axis)

Graph 7:

In fig.7, the diagram of the linear absorption coefficient in terms of photon energy for different sizes h3 (along the z-axis). It is shown below. We know that the total absorption coefficient is equal to the sum of the linear and non-linear absorption coefficients. As can be seen, with the increase in the size of the quantum dot, the energy decreases, and the absorption coefficient decreases.

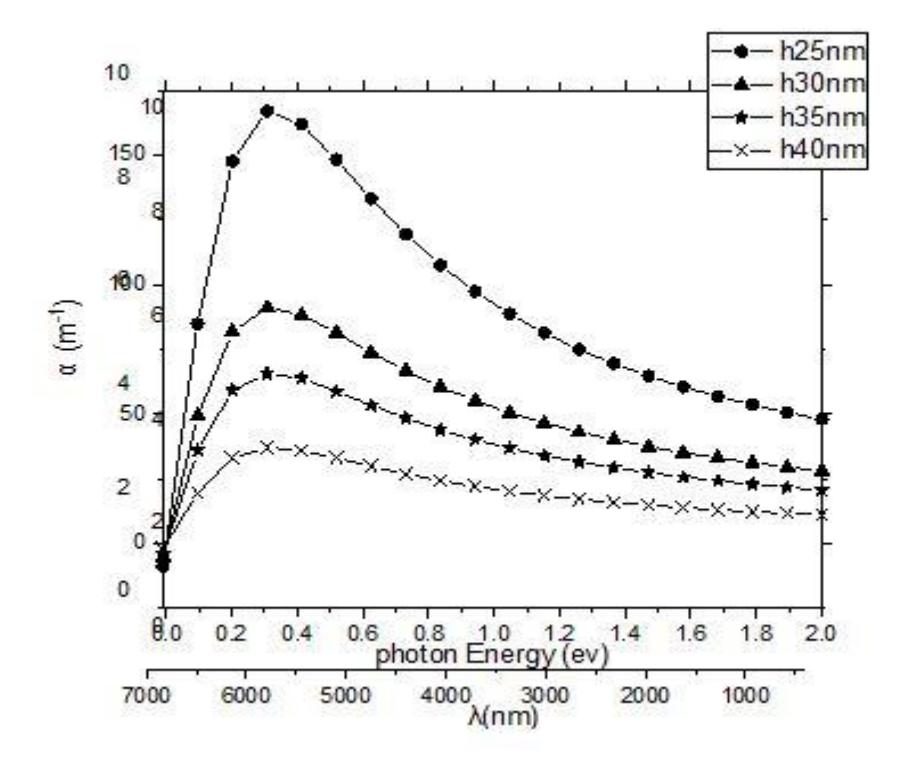


Fig. 7. The variation of linear absorption coefficients changes with the photon energy values for different sizes h3 (along the Z axis)

Graph 8:

In Fig. 8, the diagram of linear and non-linear absorption coefficient changes as a function of photon energy for different sizes h3 (along the z-axis). It is shown below. We know that the total absorption coefficient is equal to the sum of the linear and non-linear absorption coefficients. As can be seen, with the increase in the size of the quantum dot, the energy decreases, and the absorption coefficient decreases.

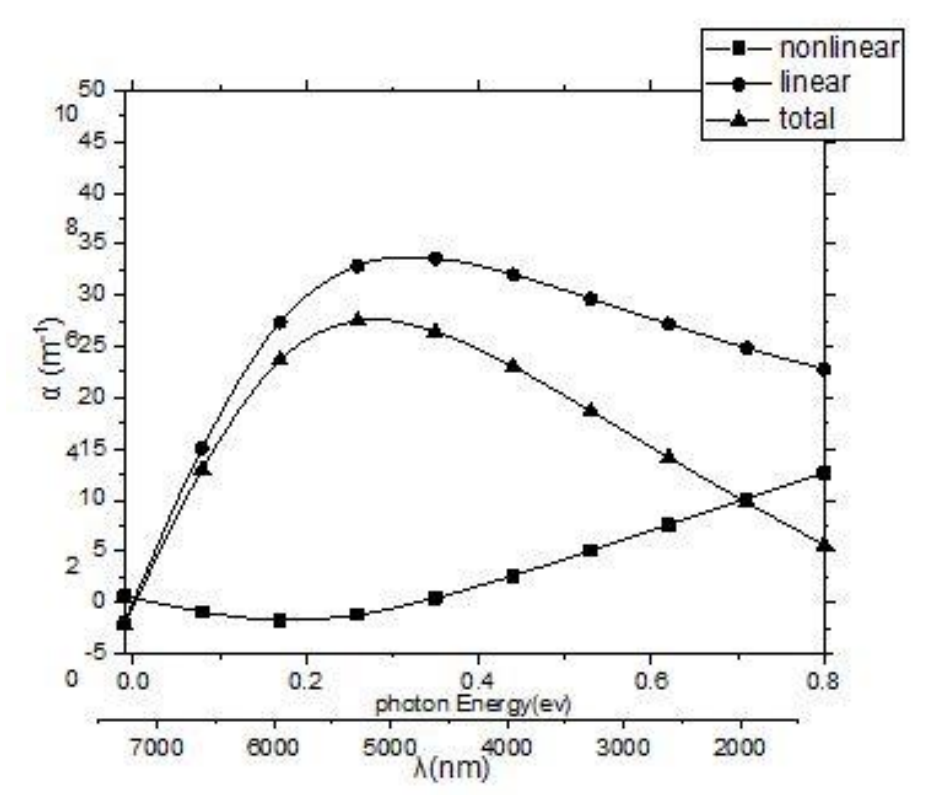


Fig. 8. The variation of linear, third-order, and total absorption coefficients change with the photon energy values for different sizes h3 (along the Z axis)

4. CONCLUSION

In summary, analytical formulations for linear and third-order nonlinear optical properties of quantum dots were developed using the compact density matrix method. The investigation highlights the sensitivity of inter-subband optical responses to the geometrical and compositional parameters of the quantum dot. It was found that linear variations in absorption and refractive index are largely independent of the optical excitation intensity [30], whereas the third-order nonlinear contributions are strongly intensity-dependent. Increasing the optical field strength was shown to reduce the overall absorption coefficient. The behavior of the linear, nonlinear, and third-order absorption coefficients with respect to photon energy and optical intensity exhibits close similarity to that observed in quantum well systems [23]. These findings are expected to provide

useful guidance for experimental verification as well as for further theoretical development. Moreover, the enhanced absorption in the visible and infrared regions demonstrates the potential of such quantum dot structures for high-performance optoelectronic devices such as photodiodes and solar energy converters [29].

References

- [1]. Rahimi F, Ghaffary T, Naimi Y, Khajehazad H. Study of the energy states and absorption coefficients of quantum dots and quantum anti-dots with hydrogenic impurity under applied magnetic field. J Optoelectron Nanostruct. 2022;7(1):1–18. https://doi:10.30495/jopn.2021.28784.1232.
- [2] Bhatt V, Yadav S. Optical response in a double quantum dot molecule inside a nonlinear photonic crystal cavity. *Photonics Nanostruct.* 2022;51:101043. http://doi:10.1016/j.photonics. 2022.101043.
- [3]. Zekavat Fetrat M, Sabaeian M, Solookinejad G. Effect of ambient temperature on linear and nonlinear optical properties of truncated pyramidal-shaped InAs/GaAs quantum dot. J Optoelectron Nanostruct. 2021;6(3):81–92. https://doi:10.30495/jopn.2021.29138.1240.
- [4]. Brahim T, Bouazra A, Said M. Linear and nonlinear optical responses of a core—shell spherical quantum dot with impurity under magnetic field. Opt Quant Electron. 2024;56:1462. https://doi:10.1007/s11082-024-07373-9.
- [5]. Gutiérrez-Fuentes R, Jiménez-Pérez JL, García-Vidal OU, et al. Theoretical study of excitonic states and optical absorption in semiconductor nanostructures. J Mater Sci Mater Electron. 2024;35:1216–1225. https://doi:10.1007/s10854-024-12993-8.
- [6]. Leshko RY, Leshko OV, Bilynskyi IV, Holskyi VB. Magneto-optical absorption in spherical quantum dots with central impurity. Opt Commun. 2024;566:130722. https://doi:10.1016/j.optcom.2024.130722.
- [7]. Assafrão D, de Lima AG, Silva EO, Filgueiras C. Magnetic and electric field effects on hydrogenic impurity states in quantum dots. Physica B Condens Matter. 2025;714:417474. https://doi:10.1016/j.physb.2025.417474.
- [8]. Cai Y, et al. Theoretical analysis of confined states in spherical semiconductor quantum dots. Phys Scr. 2025;100:065957. https://doi:10.1088/1402-4896/add589.
- [9]. Esaki L, Tsu R. Superlattice and negative differential conductivity in semiconductors. IBM J Res Dev. 1970;14:61–65. https://doi:10.1147/rd.141.0061.
- [10]. Zhang L, Xie HJ. Electronic states and optical properties of quantum dots under magnetic field. Phys Rev B. 2003;68:235315. https://doi:10.1103/PhysRevB.68.235315.
- [11]. Karabulut I, Atav U, Safak H. Comment on "Magnetic field effects in quantum dots". Phys Rev B. 2005;72:207301. https://doi:10.1103/PhysRevB.74.153306.
- [12]. Karabulut I, Safak HS, Tomak M. Linear and nonlinear optical properties of quantum dots with impurity. Solid State Commun. 2005;135:735–740. https://doi:10.1016/j.ssc.2005.06.001.
- [13]. Karabulut I, Safak HS. Temperature dependence of optical absorption in quantum dots. Physica B. 2005;368:82–86. https://doi:10.1016/j.physb.2005.06.040.

- [14]. Gurnick MK, DeTemple TA. Resonant tunneling in semiconductor heterostructures. IEEE J Quantum Electron. 1983;19:791–796. https://doi:10.1109/JOE.1983.1071927.
- [15]. Fejer MM, et al. Nonlinear optical interactions in periodically poled materials. Phys Rev Lett. 1989;62:1041–1044. https://doi:10.1103/PhysRevLett.62.1041.
- [16]. Takagahara T. Excitonic optical nonlinearities in quantum confined structures. Phys Rev B. 1987;36:9293–9305. https://doi:10.1103/PhysRevB.36.9293.
- [17]. Sauvage S, et al. Confinement and optical transitions in self-assembled quantum dots. Phys Rev B. 1999;59:9830–9835. https://doi:10.1103/PhysRevB.59.9830.
- [18]. Brunhes T, et al. Quantum size and strain effects in InAs/GaAs quantum dots. Phys Rev B. 2000;61:5562–5566. https://doi:10.1103/PhysRevB.61.5562.
- [19]. Kan Y, et al. Temperature-dependent characteristics of resonant tunneling diodes. IEEE J Quantum Electron. 1987;23:2167–2171. https://doi:10.1109/JQE.1987.1073288.
- [20]. Ahn D, Chuang SL. Effects of nonparabolicity and band mixing in quantum wells. IEEE J Quantum Electron. 1987;23:2196–2203. https://doi:10.1109/JOE.1987.1073280.
- [21]. Chuang SL, Ahn D. Band structure and optical transitions in semiconductor superlattices. J Appl Phys. 1989;65:2822–2827. https://doi:10.1063/1.342719.
- [22]. Shi JJ, Pan SH. Energy levels and optical transitions in finite superlattices. Superlattice Microstruct. 1995;17:91–96. https://doi:10.1063/1.342719.
- [23]. Kuhn KJ, et al. Quantum confinement effects in semiconductor heterostructures. J Appl Phys. 1991;70: 5010–5015. https://doi:10.1063/1.349005.
- [24]. Karabulut I, Unlu S, Safak HS. Optical absorption in quantum dots with donor impurity. Phys Status Solidi B. 2005;242: 2902–2906. https://doi:10.17714/gumusfenbil.403764.
- [25]. Zekavat MA, Sabaeian M, Solookinejad G. Effect of ambient temperature on linear and nonlinear optical properties of truncated pyramidal-shaped InAs/GaAs quantum dot. J Optoelectron Nanostruct. 2021; 6(3):81–92. https://doi:10.30495/JOPN.2021.29138.1240.
- [26]. Bera D, Qian L, Tseng TK, Holloway PH. Quantum Dots and Their Multimodal Applications: A Review. Materials (Basel) .2010;3(4):2260–2345. https://doi:10.3390/ma3042260.
- [27] Lodahl P, Mahmoodian S, Stobbe S. Interfacing single photons and single quantum dots with photonic nanostructures. Rev Mod Phys. 2015;87(2):347–400. https://doi:10.1103/RevModPhys.87.347.
- [28]. Ahn D, Chuang SL. Intersubband optical absorption in a quantum well with an applied electric field. Phys Rev B. 1987;35(8):4149–4151. https://doi:10.1103/PhysRevB.35.4149
- [29] García de Arquer FP, Armin A, Meredith P, Sargent EH. Semiconductor quantum dots: Technological progress and challenges. Science. 2021;373(6561):eaz8541. https://doi:10.1126/science.aaz8541
- [30] Bagheri, M., & Izadneshan, H. (2025). Calculation of refractive index changes and intersubband optical absorption coefficients in a pyramidal quantum dot. Journal of Nonlinear Optical Physics & Materials. https://doi.org/10.1142/S0218863525500195